Cardiovascular Research (2016) **110**, 227–237
doi:10.1093/cvr/cvw048

Kcne2 deletion attenuates acute post-ischaemia/reperfusion myocardial infarction

Zhaoyang Hu[1]*, Shawn M. Crump[2], Ping Zhang[1], and Geoffrey W. Abbott[2]*

[1]Laboratory of Anesthesiology and Critical Care Medicine, Translational Neuroscience Center, West China Hospital, Sichuan University, Chengdu, Sichuan 610041, China; and [2]Bioelectricity Laboratory, Department of Pharmacology and Department of Physiology and Biophysics, School of Medicine, University of California, Irvine, CA, USA

Received 5 February 2014; revised 23 February 2016; accepted 28 February 2016; online publish-ahead-of-print 6 March 2016

Time for primary review: 34 days

Aims Most cardiac arrhythmia-associated genes encode ion channel subunits and regulatory proteins that are also expressed outside the heart, suggesting that diseases linked to their disruption may be multifactorial. KCNE2 is a ubiquitously expressed potassium channel β subunit associated with cardiac arrhythmia, atherosclerosis, and myocardial infarction (MI) in human populations. Here, we tested the hypothesis that *Kcne2* disruption in mice would influence the acute outcome of experimentally induced MI.

Methods and results One-year-old male *Kcne2*$^{+/+}$ and *Kcne2*$^{-/-}$ mice were subjected to cardiac ischaemia/reperfusion injury (IRI) by left anterior descending coronary artery ligation. After reperfusion (3 h), infarct size and markers of tissue damage were quantified. Unexpectedly, post-reperfusion, *Kcne2*$^{-/-}$ mice exhibited 40% lower infarct size, decreased myocardial apoptosis and damage, and more than two-fold lower serum levels of damage markers, lactate dehydrogenase and creatine kinase, than *Kcne2*$^{+/+}$ mice. *Kcne2* deletion, despite increasing normalized heart weight and prolonging baseline QT_c by 70%, helped preserve post-infarct cardiac function (quantified by a Millar catheter), with parameters including left ventricular maximum pressure, max d*P*/d*t* ($P < 0.01$), contractility index, and pressure/time index ($P < 0.05$) all greater in *Kcne2*$^{-/-}$ compared with *Kcne2*$^{+/+}$ mice. Western blotting indicated two-fold-increased glycogen synthase kinase 3β (GSK-3β) phosphorylation (inactivation) before and after IRI ($P < 0.05$) in *Kcne2*$^{-/-}$ mice compared with *Kcne2*$^{+/+}$ mice. GSK-3β inhibition by SB216763 mimicked in *Kcne2*$^{+/+}$ mice the cardioprotective effects of *Kcne2* deletion, but did not further enhance them in *Kcne2*$^{-/-}$ mice, suggesting that GSK-3β inactivation was a primary cardioprotective mechanism arising from *Kcne2* deletion.

Conclusions *Kcne2* deletion preconditions the heart, attenuating the acute tissue damage caused by an imposed IRI. The findings contribute further evidence that genetic disruption of arrhythmia-associated ion channel genes has cardiac ramifications beyond abnormal electrical activity.

Keywords Potassium channel • Myocardial infarction • Long QT syndrome

1. Introduction

Cardiovascular disease remains the biggest health challenge of the 21st century in developed countries. The two primary lethal events that can arise from cardiovascular dysfunction are myocardial infarction (MI) and sudden cardiac death (SCD). While multiple genetic and environmental risk factors contribute to most forms of heart disease, and dictate the incidence of MI and SCD, in some (especially younger) individuals, it is possible to link occurrence of SCD tightly with inherited or sporadic mutations in genes encoding ion channels or the proteins that regulate them.

Of the 25 genes currently known to be associated with cardiac rhythm disturbances, all encode ion channels or their regulatory subunits. Mutations in these genes can predispose to cardiac rhythm disturbances including long QT syndrome (LQTS), which in turn increases the risk of torsades de pointe, ventricular fibrillation, and SCD.[1] Arrhythmia-associated genes are typically also expressed outside the heart, raising the possibility that SCD linked to their dysfunction could

* Corresponding author. Laboratory of Anesthesiology and Critical Care Medicine, Translational Neuroscience Center, West China Hospital, Sichuan University, Chengdu, Sichuan 610041, China. Tel: +86 28 85164039; fax: +86 28 85423593, E-mail: zyhu@hotmail.com (Z.H.); 360 Medical Surge II, Department of Pharmacology, School of Medicine, University of California, Irvine, CA 92697, USA. Tel: +1 949 824 3269; fax: +1 949 824 4855, E-mail: abbottg@uci.edu (G.W.A.).

be multifactorial, and provide an ischaemic substrate as well as an electric substrate.[2–5]

Voltage-gated potassium (K_v) channels are essential for timely repolarization of cardiac myocytes, and inherited or pharmacological disruption of their function can lead to potentially lethal cardiac rhythm disturbances, creating an electrical substrate for SCD.[1] *KCNE2* encodes a relatively promiscuous K_v channel β subunit expressed in human and mouse heart and required for normal cardiac rhythm in both species.[6–11] Aside from its contribution to cardiomyocyte currents, *KCNE2* is also expressed in multiple epithelia. We previously found that, consequently, *Kcne2* deletion in mice causes a multisystem syndrome that adversely impacts the heart, generating both electrical disturbances and creating an ischaemic substrate.[5]

Interestingly, a single-nucleotide polymorphism (SNP) near the human *KCNE2* gene has been linked to early-onset MI,[12] and one within the KCNE2 gene itself is associated with predisposition to coronary artery disease (CAD)[13] and MI.[14] In addition, *Kcne2* deletion in mice promotes atherosclerosis as well as western diet-dependent ventricular arrhythmogenesis and sudden death.[15] In summary, these findings support a causal relationship between KCNE2 disruption, CAD, and MI, and suggest that KCNE2 disruption is a genetic commonality between two seemingly distinct clinical entities, SCD and MI. Here, employing the *Kcne2*$^{-/-}$ mouse model, we examined the potential influence of *Kcne2* deletion on an experimentally imposed acute ischaemic event. Surprisingly, we discovered that *Kcne2* deletion protects the heart from damage during the early post-ischaemic phase, reducing infarct size, and preserving cardiac function compared with wild-type mice.

2. Methods

2.1 Animal use

We generated and genotyped *Kcne2*$^{+/+}$ and *Kcne2*$^{-/-}$ C57BL/6 mice as previously described,[8,11] and housed and used them according to the US National Institutes of Health *Guide for the Care and Use of Laboratory Animals*. Animal procedures were approved by the Animal Care and Use Committee at the University of California, Irvine. All mice used in this study, aside from breeding females, were male, 12–14 months of age, and generated from *Kcne2*$^{+/-}$ × *Kcne2*$^{+/-}$ crosses.

2.2 Surgical procedures

Anaesthesia was induced with 5% isoflurane and 95% oxygen in a gas chamber, followed by tracheotomy and ventilation with 2% isoflurane and 98% oxygen for maintenance in a mouse ventilator (Harvard Apparatus, Holliston, MA, USA). The depth of anaesthesia and its adequacy were monitored by their heart rate, respiration rate, the loss of corneal reflex, and the absence of pedal withdrawal upon toe pinching. For analgesia and minimizing pain caused by surgical procedures, mice were given buprenorphine (0.1 mg/kg) subcutaneously. Mice were euthanized by cervical dislocation under anaesthesia at the end of the experiment. During surgery and ischaemia/reperfusion injury (IRI), mice were ventilated with a tidal volume of 250 μL at a rate of 150 strokes/min. After an equilibration period of 10 min, a thoracotomy was performed at the left fourth intercostal space. A prominent branch of the left anterior descending coronary artery (LAD) was identified. A 9-0 polyamide Ethilon suture (Ethicon, Somerville, NJ, USA) was passed underneath this vessel approximately halfway between the base and the apex for coronary artery occlusion. The standard limb lead II configuration electrocardiographic system was attached subcutaneously by needle electrodes. ECG was performed in anaesthetized mice using PowerLab/8sp and LabChart 7.2.1 software (AD Instruments, Colorado Springs, CO, USA) under continuous flow with isoflurane vapours. Successful arterial occlusion was verified by ECG alteration (i.e. ST-elevation) and the presence of regional dyskinesia and epicardial cyanosis in the ischaemic zone. Reperfusion was achieved by releasing the snare and was verified by observing an epicardial hyperaemic response and gradual resolution of the changes in the ECG signal. The suture was loosened after 45 min of ischaemia, and the ischaemic myocardium was reperfused for 3 h, with constant surface ECG monitoring throughout. Temperature was maintained with a heating blanket. Glycogen synthase kinase 3β (GSK-3β) inhibitor SB216763 (0.6 mg/kg; Sigma, St Louis, MO, USA) was intravenously applied to mice of either genotype 5 min prior to reperfusion injury.

2.3 Haemodynamic analyses

The portion of the right carotid artery next to the trachea was isolated from the surrounding tissue and nerves. A 1.0-Fr Millar Mikro-tip Catheter Transducer (Model SPR-1000, Millar Instruments, Houston, TX, USA) connected to a pressure transducer (Millar Instruments) was inserted through the right carotid artery into the left ventricular (LV) cavity. Haemodynamic parameters were recorded and analysed with PowerLab/8sp and LabChart 7.2.1 software. The standard limb lead II configuration electrocardiographic system was attached subcutaneously by needle electrodes for ECG studies. The corrected QT interval (QT_c) was calculated based on a variant of Bazett's formula modified specifically for mice.[16]

2.4 Quantification of myocardial infarct size and tissue injury

At the end of reperfusion, the LAD was re-occluded and the heart was perfused with 1% Evans blue dye (Sigma) to delineate the field of the occluded artery and thus identify the area at risk (AAR). After transient freezing, hearts were cut into transverse slices of equal thickness (1 mm). Triphenyltertrazolium chloride (TTC) staining was used to determine myocardial infarct size. The tissue slices were incubated with 1% TTC (Sigma Chemical Co.) in 0.1 M phosphate buffer (pH 7.4) for 20 min at 37°C. Tissues were then fixed in 10% PBS-buffered formalin overnight at room temperature. Infarcted and non-infarcted myocardium within the AAR were carefully separated and weighed. Infarct size was expressed as a percentage of the AAR. To further quantify cardiac tissue injury, serum levels of lactate dehydrogenase (LDH), creatine kinase (CK), and myoglobin were quantified at the University of California, Davis Pathology Core Facility using standard procedures.

2.5 Tissue collection

A separate group of experimental animals, parallel to that used for infarct size quantification, was used for histology and western blot analysis. At the end of 3 h reperfusion, the LAD was re-occluded and 1% Evans blue was injected into the LV to delineate the AAR zone. For histology, the whole heart including ischaemic and non-ischaemic areas was dissected and cut into slices, parallel to the atrioventricular groove in 1-mm-thick sections. The slices were rinsed in saline, briefly blotted onto filter paper to dry, and then immersed in 10% phosphate-buffered formalin solution overnight at room temperature. Heart sections were then fixed in formaldehyde, dehydrated, and embedded in paraffin. Serial sections of transverse myocardial slices (5 μM thickness), which included the LV walls and the septum from each heart, were mounted on glass slides for haematoxylin and eosin (H&E). For terminal deoxynucleotidyl transferase-mediated dUTP nick-end labelling (TUNEL) staining, serial sections of transverse myocardial slices, which included the LV walls and the septum from each heart, were mounted on glass slides for apoptosis measurement. For western blot analysis, hearts were quickly removed and the LV AAR was immediately snap-frozen.

2.6 TUNEL staining

TUNEL assay was used for apoptosis determination according to the manufacturer's protocol (Roche Diagnostics, Indianapolis, IN, USA). Ten fields

from each heart were chosen randomly and analysed in a blind manner. TUNEL-positive apoptotic nuclei were stained red and TUNEL-negative nuclei were stained blue. The apoptotic index was judged as a per cent of the number of TUNEL-positive cardiomyocyte apoptotic nuclei out of the total cardiomyocyte nuclei population. Images were obtained using the CAST system (Olympus A/S, Ballerup, Denmark) and analysed with Image-pro plus (Media Cybernetics, Inc., Carlsbad, CA, USA).

2.7 Histological evaluation of myocardial damage

A modified numerical scoring system was used in this analysis for histopathological evaluation based on a scoring system described by Ko *et al.*[17] Briefly, myocardial damage including interstitial oedema, myofibre degeneration (i.e. myofibre swelling), and subendocardial haemorrhage was graded as to their severity (0 = no damage, 1 = mild, 2 = moderate, and 3 = marked) and distribution (0 = no damage, 1 = focal damage, 2 = multifocal damage, and 3 = diffuse damage). A mean score for each variable was determined for each heart. Hearts were evaluated by LM in a double-blind manner.

2.8 Immunofluorescence detection

Ventricular tissue samples from *Kcne2*$^{+/+}$ and *Kcne2*$^{-/-}$ mice (two per genotype) were frozen, sectioned on a cryostat, then fixed, and permeabilized in ice-cold acetone for 10 min. Immunofluorescence labelling was performed manually, with 3 × 5 min washes in PBS between steps. Slides were incubated overnight at 4°C with rabbit polyclonal primary antibodies (anti-KI67 from Novus Biologicals, Littleton, CO, USA; anti-Cyclin D1 from Abcam, Cambridge, MA, USA) at 1/100 dilution in PBS with 10% BSA, followed by a 2-h dilution in Alexa-fluor 488-conjugated donkey anti-rabbit secondary antibody (ThermoFisher Scientific, Waltham, MA, USA) at 1/500 dilution in PBS. For a negative control, primary antibody was omitted. After mounting using DAPI-containing slow-fade mounting medium (Life Technologies, Grand Island, NY, USA), slides were viewed with an Olympus BX51 microscope and pictures were acquired using the CellSens software (Olympus, Waltham, MA, USA). Images used were each representative of two mice, four sections per mouse.

2.9 Western blotting

Frozen cardiac tissue was homogenized and suspended in radioimmunoprecipitation assay (RIPA) buffer containing protease inhibitor cocktail (Sigma). Homogenates were then subjected to centrifugation for 10 min at 4000 rpm. Debris was removed and the supernatant was retained. For the cardiac membrane preparation, this was followed by pelleting of membrane fractions at 40 000 × *g* for 10 min. Protein concentration was determined and normalized using the bicinchoninic acid (BCA) assay (Pierce, Rockford, IL, USA). Soluble protein fractions (20 μg) were separated on pre-cast NuPAGE 4–12% Bis-Tris gels (Invitrogen, Carlsbad, CA, USA) and were transferred to nitrocellulose membranes (Bio-Rad, Carlsbad, CA, USA). Blots were blocked for 1 h at room temperature with 5% non-fat milk in Tris-buffered saline (TBS)-Tween. Antibodies raised against extracellular signal-regulated kinases 1 and 2 (ERK1/2), phospho$^{Thr202/204}$-ERK1/2, AKT, phospho^{Ser473}-AKT, GSK-3β, phospho^{Ser9}-GSK-3β (rabbit, 1 : 1000; Cell Signaling, Danvers, MA, USA), Bcl-2, and BAX (rabbit, 1 : 1000, Santa Cruz, Dallas, TX, USA) were used for primary detection. Goat anti-rabbit IgG secondary antibody linked to horseradish peroxidase was used for chemiluminescent detection (Millipore, Billerica, MA, USA). Signals were analysed with a Gbox system using the Gbox software (Syngene, Frederick, MD, USA). Band densities were quantified using the ImageJ Data Acquisition Software (NIH, Bethesda, MD, USA).

2.10 Statistical analysis

Data were analysed with SPSS 16.0 software for Windows (SPSS, Inc., Chicago, IL, USA), Graphpad Prism 5 software (La Jolla, CA, USA), or Microsoft Excel (Seattle, WA, USA). Values are presented as the mean ± SEM. The statistical test for ST-segment changes over time was performed by two-way repeated-measures ANOVA. Comparison of two means was performed using an unpaired Student's *t*-test. Comparison of several means was performed using one-way ANOVA. If variances determined by homogeneity-of-variance assumption were equal, the Bonferroni test was examined *post hoc* for multiple comparisons; otherwise, the Dunnett's T3 test was applied. All *P*-values were two-tailed. Statistical significance was defined as $P < 0.05$.

3. Results

3.1 *Kcne2* deletion attenuates acute MI and cardiac tissue damage after IRI

Normalized AAR and infarct size were quantified in *Kcne2*$^{+/+}$ and *Kcne2*$^{-/-}$ mice subjected to 45 min of LAD occlusion followed by 180 min of reperfusion. The ratio of the AAR to the left ventricle was similar between *Kcne2*$^{+/+}$ and *Kcne2*$^{-/-}$ mice ($P = 0.22$, *Figure 1A* and *B*). In contrast, infarct size (calculated as the percentage of the AAR) was significantly smaller in *Kcne2*$^{-/-}$ mice (28 ± 4% of AAR) than in *Kcne2*$^{+/+}$ mice (45 ± 5% of AAR; $P < 0.05$, $n = 5–6$, *Figure 1C*).

Also indicative of less post-IRI cardiac tissue damage in *Kcne2*$^{-/-}$ mice compared with *Kcne2*$^{+/+}$ mice, *Kcne2*$^{+/+}$ mice exhibited 4.3-fold higher serum CK and 2.0-fold higher serum LDH than *Kcne2*$^{-/-}$ mice, post-reperfusion ($P < 0.01$ or < 0.001, $n = 10–12$; *Figure 1D* and *E*). However, there was no difference in post-IRI serum myoglobin level between the two genotypes ($P = 0.61$, $n = 7–8$; *Figure 1F*). There was a ∼40% higher Bcl-2/BAX ratio in post-IRI ventricular tissue from *Kcne2*$^{-/-}$ mice compared with that of *Kcne2*$^{+/+}$ mice, suggestive of relatively less apoptosis in the former in response to IRI. However, this did not reach statistical significance because of variability within the *Kcne2*$^{-/-}$ mouse group ($P = 0.38$, $n = 6–7$; *Figure 1G*). Consistent with this, after 3 h reperfusion, TUNEL-positive cells were detected within the left ventricles in both genotypes; however, the ratio of apoptotic cardiomyocytes to the total number of cardiomyocytes was significantly reduced in *Kcne2*$^{-/-}$ mouse ventricles compared with their wild-type littermates ($P = 0.0002$, *Figure 1H*). Myocardial damage was also evaluated by H&E staining and quantification was also evaluated using a previously described histological scoring system.[17] LV tissue after IRI in both genotypes suffered various degrees of myocyte injury, including steatosis, subendocardial haemorrhage, oedema, and vacuolization. Compared with *Kcne2*$^{+/+}$ mice, the degree of myocardial injury was less severe in *Kcne2*$^{-/-}$ hearts ($P = 0.02$). While these cardiac morphological changes spread to larger zones of the myocardium, necrosis was not detected in either group (*Figure 1I*).

3.2 *Kcne2* deletion helps to preserve cardiac function after IRI

Suggestive of similar levels of ischaemia between genotypes, ECG analysis showed similar ST-segment changes throughout the LAD ligation and reperfusion periods between these two genotypes (*Figure 2A–D*). *Kcne2* deletion helped to preserve cardiac function post-IRI. At baseline, *Kcne2* deletion had no effects on LV pressure and other functional parameters (*Figure 2E–H* and see Supplementary material online, *Figure*

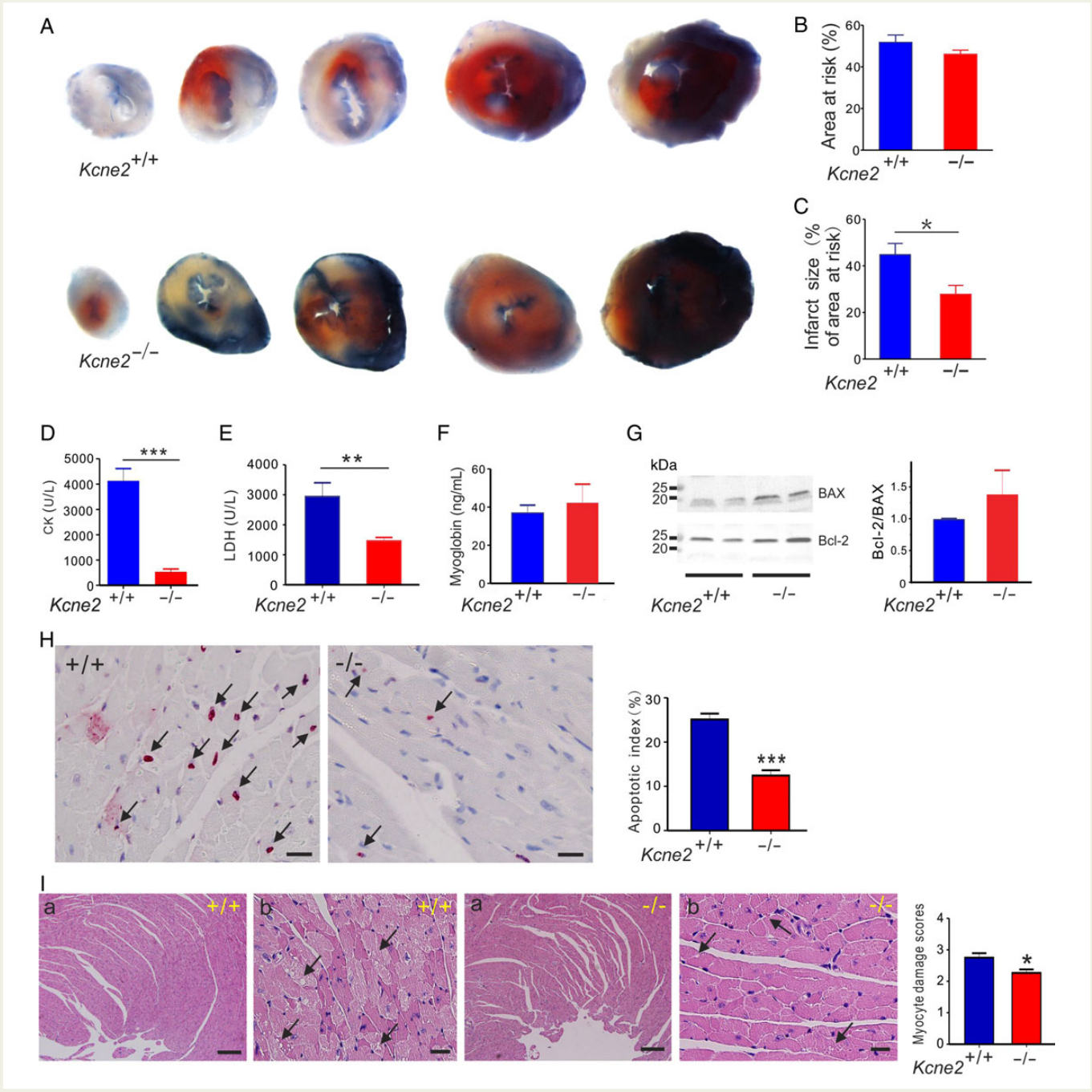

Figure 1 *Kcne2* deletion decreases infarct size and cardiac damage after experimentally imposed IRI. (*A*) Representative photographs of Evans blue-perfused, TTC-stained heart sections obtained from $Kcne2^{+/+}$ and $Kcne2^{-/-}$ mice. Red, AAR; blue, healthy viable tissue; white, infarcted tissue. (*B*) Mean AAR after IRI expressed as a percentage of LV area in $Kcne2^{+/+}$ and $Kcne2^{-/-}$ mice. ($n = 5–6$ per group). (*C*) Mean myocardial infarct size after IRI expressed as a percentage of the LV AAR in $Kcne2^{+/+}$ and $Kcne2^{-/-}$ mice ($n = 5–6$ per group). $^{*}P < 0.05$ between genotypes. (*D*) Post-IRI mean serum levels of CK of $Kcne2^{+/+}$ and $Kcne2^{-/-}$ mice ($n = 10–11$). $^{***}P < 0.001$ between genotypes. (*E*) Post-IRI mean serum levels of LDH of $Kcne2^{+/+}$ and $Kcne2^{-/-}$ mice ($n = 12$). $^{**}P < 0.01$ between genotypes. (*F*) Post-IRI mean serum levels of myoglobin of $Kcne2^{+/+}$ and $Kcne2^{-/-}$ mice ($n = 7–8$). (*G*) Left: representative western blots showing post-IRI ventricular BAX and Bcl-2 expression, one mouse per lane. Right: mean band density from blots as in left, $n = 6–7$. (*H*) Left: representative TUNEL-stained heart sections of mice subjected to 45 min of myocardial ischaemia and 3 h of reperfusion injury. Arrows indicate TUNEL-positive cardiomyocytes (red). Scale bars, 10 μm. Right: graph showing the averaged percentage of TUNEL-positive cells in the ischaemic regions of LVs ($n = 4–5$, each genotype). $^{***}P < 0.001$ between genotypes. (*I*) Left: representative histological H&E-stained micrographs of cardiac section including the ischaemic and the non-ischaemic areas of the LV tissue from $Kcne2^{+/+}$ and $Kcne2^{-/-}$ mice as indicated, representative of $n = 4–6$ mice per genotype. Arrows point at either myocyte cytoplasmic vacuolation, oedema, haemorrhage, or steatosis. Panel (a) scale bars: 100 μm; panel (b) scale bars, 10 μm. Right: morphological evaluation of myocardium damage after reperfusion in ischaemic left ventricles of both genotypes ($n = 4–6$ mice per genotype). The type and severity of myocardial lesions were graded from 0 to 3 (see the 'Methods' section). $^{*}P < 0.05$ between genotypes.

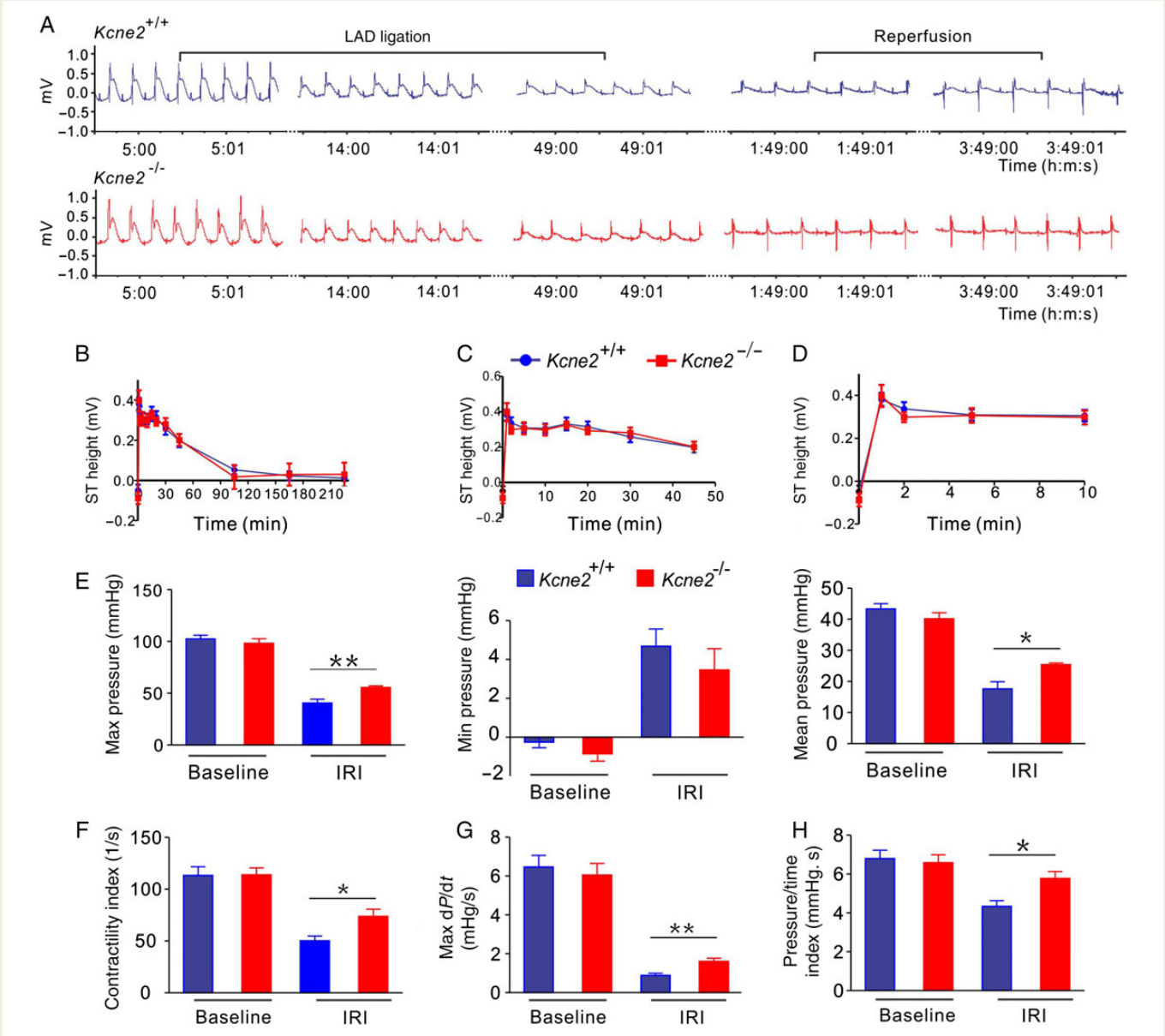

Figure 2 *Kcne2* deletion attenuates loss of cardiac contractile function after experimentally imposed IRI. (*A*) Exemplar LAD ligation and reperfusion of ECG traces from *Kcne2*$^{+/+}$ and *Kcne2*$^{-/-}$ mice ($n = 12–18$/genotype). (*B*) Mean ST heights during 45 min of LAD ligation and 3 h of reperfusion in *Kcne2*$^{+/+}$ and *Kcne2*$^{-/-}$ mice quantified from ECG traces as in *A* ($n = 12–18$). Groups were not significantly different (by repeated-measures ANOVA). (*C*) Mean ST heights during 45 min of LAD ligation in *Kcne2*$^{+/+}$ and *Kcne2*$^{-/-}$ mice quantified from ECG traces as in *A* ($n = 12–18$). (*D*) Mean ST heights during the first 10 min of LAD ligation in *Kcne2*$^{+/+}$ and *Kcne2*$^{-/-}$ mice quantified from ECG traces as in *A* ($n = 12–18$). (*E*) Maximum, minimum, and mean LV pressure parameters measured in *Kcne2*$^{+/+}$ (blue) and *Kcne2*$^{-/-}$ (red) mice with a Millar catheter before (baseline, $n = 10–13$) and after (IRI, $n = 5–6$) 45 min of LAD occlusion followed by 180 min of reperfusion. *$P < 0.05$ between genotypes; **$P < 0.01$ between genotypes. (*F*) Contractility index for mice as in *E*; *$P < 0.05$ between genotypes. (*G*) Rate (max d*P*/d*t*) of LV pressure rise in early systole for mice as in *E*; **$P < 0.01$ between genotypes. (*H*) Pressure/time index for mice as in *E*; *$P < 0.01$ between genotypes.

S1). IRI produced an expected loss of pressure and contractility in mice of either genotype, but was much less impactful on *Kcne2*$^{-/-}$ mice, again indicative of the protective effect of *Kcne2* deletion against early post-infarct myocardial tissue damage in the context of experimentally imposed IRI. Thus, compared with post-IRI *Kcne2*$^{+/+}$ mice, post-IRI *Kcne2*$^{-/-}$ mice showed 50–100% greater maximum LV pressure, maximum–minimum pressure, isovolumic relaxation period d*P*/d*t*, maximum d*P*/d*t* (all $P < 0.01$), contractility index, pressure/time index, mean LV pressure, and minimum d*P*/d*t* (all $P < 0.05$; baseline, $n = 10–13$; IRI, $n = 5–6$, *Figure 2E–H* and see Supplementary material online, *Figure S1*).

3.3 *Kcne2* deletion stimulates baseline cardiac remodelling and GSK-3β phosphorylation

The greater preservation of cardiac function in *Kcne2*$^{-/-}$ mice compared with age-matched wild-type mice post-IRI was particularly

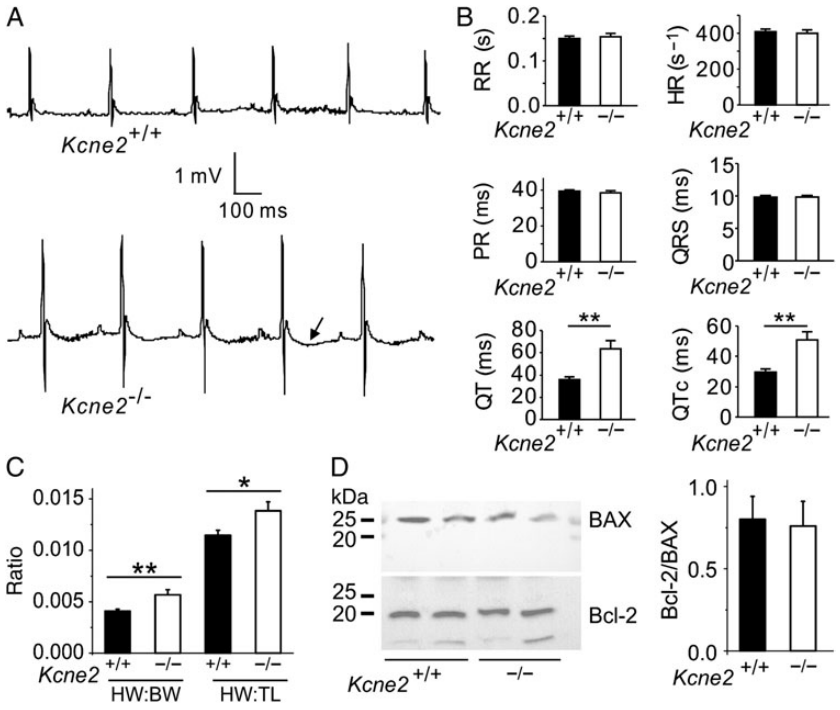

Figure 3 *Kcne2* deletion stimulates baseline cardiac remodelling. (*A*) Representative surface ECG traces from *Kcne2*$^{+/+}$ and *Kcne2*$^{-/-}$ mice showing prolonged T wave (arrow) in the latter ($n = 12–17$ each genotype). (*B*) Actual ECG parameters measured from mice ($n = 12–17$) showing QT and QTc prolongation in *Kcne2*$^{-/-}$ mice. $^{**}P < 0.01$. All other group comparisons $P > 0.05$. HR, heart rate; PR, PR interval; RR, RR interval. (*C*) Mean heart-weight to body-weight (HW:BW) and heart-weight to tibia-length (HW:TL) measurements for *Kcne2*$^{+/+}$ and *Kcne2*$^{-/-}$ mice ($n = 13–17$). $^{*}P < 0.05$ between genotypes; $^{**}P < 0.01$ between genotypes. (*D*) Left: representative western blots showing baseline ventricular BAX and Bcl-2 expression, one mouse per lane. Right: mean band density from blots as in left, $n = 6$ per genotype.

noteworthy given the evidence of extensive electrical and structural remodelling occurring at baseline (i.e. in the absence of experimentally induced IRI) in *Kcne2*-deleted myocardium. This included a 76% longer QT interval and 71% longer QT_c (*Figure 3A* and *B*; $n = 12–17$) and 38% greater normalized heart weight (*Figure 3C*) in *Kcne2*$^{-/-}$ mice compared with *Kcne2*$^{+/+}$ mice. There was no difference in baseline ventricular tissue apoptotic activity between the two genotypes, as indicated by equal Bcl-2/BAX protein ratios (*Figure 3D*). In contrast, there were genotype-dependent differences in phosphorylation of proteins known to be involved in signalling cascades activated in response to ischaemic damage. Thus, the ratio of phosphorylated (p) to total (t) GSK-3β at baseline in *Kcne2*$^{-/-}$ mice was almost double that of *Kcne2*$^{+/+}$ mice either in whole ventricles ($P = 0.047$, *Figure 4A*) or ventricular myocyte membrane fractions (see Supplementary material online, *Figure S2A*). Similarly, the ratio of pGSK-3β to total tGSK-3β in *Kcne2*$^{-/-}$ mice post-IRI was double that of *Kcne2*$^{+/+}$ mice ($P < 0.01$, *Figure 4A*, or $P < 0.05$, see Supplementary material online, *Figure S2A*). We also observed 50% increased ERK1/2 phosphorylation in *Kcne2*$^{-/-}$ mouse ventricular lysates and in ventricular membrane fractions, only at baseline, but this did not achieve statistical significance ($P > 0.05$), and we saw no difference in the ratio of phosphorylated to total protein kinase B (AKT), between genotypes either before or after IRI (*Figure 4B* and *C*, see Supplementary material online, *Figure S2B* and *C*).

3.4 Inhibition of GSK-3β mimics the cardioprotective effect of *Kcne2* deletion against reperfusion injury

To further explore the respective roles of GSK-3β in *Kcne2* deletion-induced infarct size limitation, we applied GSK-3β inhibitor SB216763 after the LAD occlusion but 5 min prior to cardiac reperfusion. It is well established that GSK-3β inhibitors reduce infarct size; we therefore examined whether SB216763 treatment would affect *Kcne2* deletion-linked cardioprotection. The ratio of the AAR to the left ventricle was similar among groups ($P > 0.05$). Infarct sizes were calculated as percentages of the AAR and were also comparable among groups. Inhibition of GSK-3β activity with SB216763 in the *Kcne2*$^{+/+}$ and *Kcne2*$^{-/-}$ mice resulted in similar infarct sizes to those observed in *Kcne2*$^{-/-}$ mice in the absence of SB216763, i.e. reduced compared with non-SB216763-treated *Kcne2*$^{+/+}$ mice ($P < 0.05$; *Figure 5A* and *B*). SB216763 decreased *Kcne2*$^{+/+}$ mouse serum LDH and CK, compared with untreated *Kcne2*$^{+/+}$ mice, to levels similar to that of untreated *Kcne2*$^{-/-}$ mice, but did not alter serum CK or LDH levels in *Kcne2*$^{-/-}$ mice; the serum concentration of CK-MB after IRI was unaffected by SB216763 in either genotype (*Figure 5C*). Expressed as a percentage of total normal nuclei, SB216763 halved the degree of apoptosis in *Kcne2*$^{+/+}$ mice, but did not further reduce that observed in *Kcne2*$^{-/-}$ mouse ventricles (*Figure 5D*). Meanwhile, pretreatment of SB216763 also decreased post-I/R myocardial damage, compared with

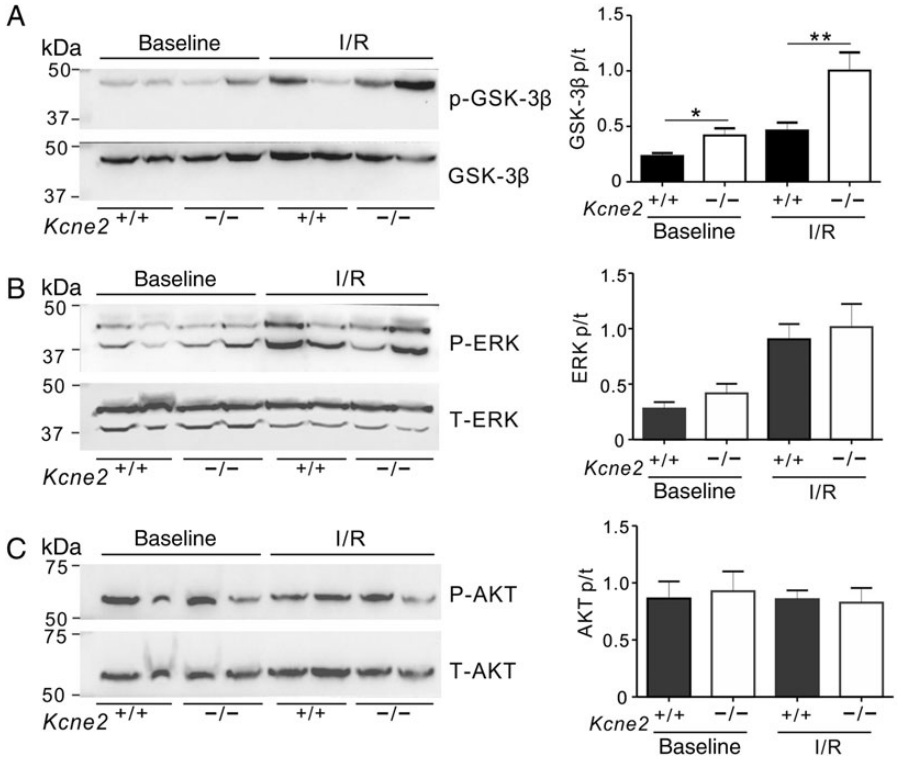

Figure 4 *Kcne2* deletion increases ventricular GSK-3β phosphorylation. (*A*) Left: representative western blots showing baseline and post-IRI ventricular phospho- (p-) GSK-3β and total (t) GSK-3β expression, one mouse per lane. Right: mean ratio of pGSK-3β/tGSK-3β band density from blots as in left; $n = 4–6$; $^{*}P < 0.05$, $^{**}P < 0.01$ between genotypes. (*B*) Left: representative western blots showing baseline and post-IRI ventricular phospho- (p-) ERK1/2 and total (t) ERK1/2 expression, one mouse per lane. Right: mean ratio of pERK/tERK band density from blots as in left; $n = 4–6$. (*C*) Left: representative western blots showing baseline and post-IRI ventricular phospho- (p-) AKT and total (t) AKT expression, one mouse per lane. Right: mean ratio of pAKT/tAKT band density from blots as in left; $n = 4–6$.

non-SB216763-treated *Kcne2*$^{+/+}$ mice, as assessed by histological scoring of myocyte morphology, resulting in equivalent myocyte damage in either genotype, and to a degree similar to that of *Kcne2*$^{-/-}$ hearts without inhibitor ($P = 0.027$, see Supplementary material online, *Figure S3*).

3.5 Pharmacological inhibition of GSK-3β mimics effects of *Kcne2* deletion on GSK-3β phosphorylation

GSK-3β inhibition in *Kcne2*$^{+/+}$ mice by SB216763 also mimicked the effects of *Kcne2* deletion (*Figure 4A*) on ventricular GSK-3β phosphorylation ($P < 0.001$, *Figure 6A*) while not further altering GSK-3β phosphorylation in *Kcne2*$^{-/-}$ mouse ventricles (*Figure 6A*). SB216763 did not further alter phosphorylation of ERK1/2, which was elevated in post-IRI mice compared with baseline mice regardless of genotype, or of AKT, which was unaffected by IRI (*Figure 6B* and *C*).

4. Discussion

Kcne2-deficient mice exhibit a higher risk for cardiac events compared with their wild-type littermates, arising from one or more of a battery of risk factors including LQTS, increased heart weight, elevated serum angiotensin II, lipid accumulation, impaired glucose tolerance, and hyperkalaemia.[5] In addition, mirroring the association of *KCNE2* sequence variants with CAD and MI in human populations,[12–14,18] *Kcne2* deletion promotes atherosclerosis in mice.[15] Here, we were therefore initially surprised to find that *Kcne2* deletion was cardioprotective in the early post-IRI period following LAD ligation in mice.

Compared with mid- or distal-LAD infarction, human individuals with a proximal LAD infarction are associated with a higher incidence of arrhythmias and cardiac death. Accordingly, experimental animal studies have repeatedly shown that animal mortality and infarct size increases as the distance of the ligation from the origin of the LAD decreases.[19] Previously, we discovered that *Kcne2* deletion predisposes to SCD because its disruption can generate both electric and ischaemic substrates, and a trigger for SCD.[5] In those studies, we used a ligation protocol with a higher, close-to-origin LAD ligation for 10 min, imposing an aggressive, short-lived ischaemia to uncover early reperfusion-induced arrhythmogenesis. In that context, *Kcne2* deletion was deleterious, predisposing to ventricular fibrillation and SCD within the first 20 min of reperfusion. In the current study, we ligated the LAD lower down (albeit for longer) to create a less aggressive ischaemic insult. With this protocol, none of the mice of either genotype experienced sustained ventricular tachycardia or ventricular fibrillation; all survived the full 3 h of reperfusion, permitting us to examine outcomes with respect to infarct size in this early phase of reperfusion. In contrast to the effects of reperfusion-induced arrhythmogenesis in our prior study, here we found that *Kcne2* deletion was cardioprotective in the

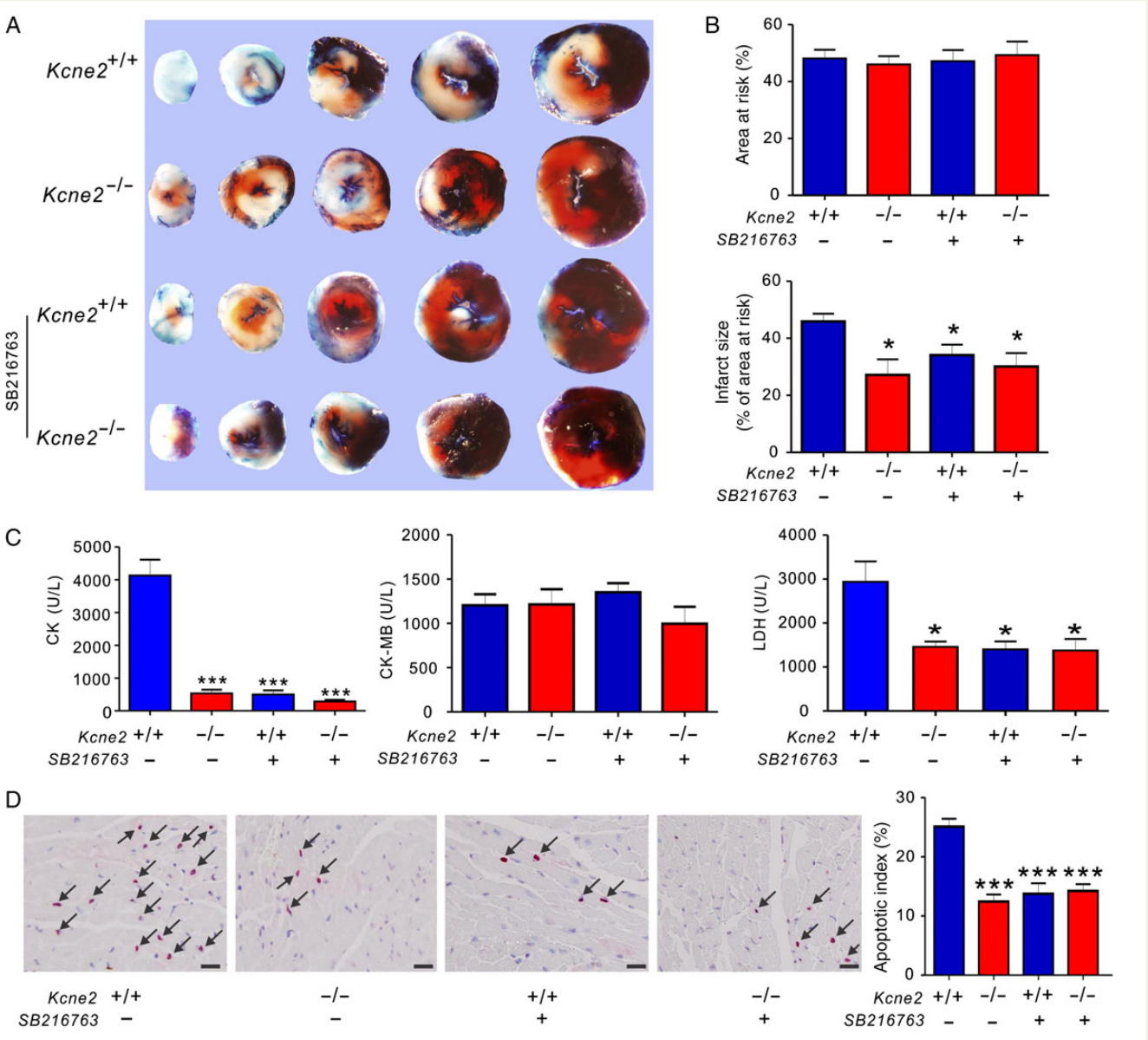

Figure 5 The effect of pharmacological inhibition of GSK-3β upon reperfusion in *Kcne2*$^{+/+}$ and *Kcne2*$^{-/-}$ mice. (*A*) Representative TTC-stained sections isolated from *Kcne2*$^{+/+}$ and *Kcne2*$^{-/-}$ mouse hearts subjected to 45 min of LAD ligation followed by 180 min of reperfusion in the presence (+) or absence (−) of SB216763. (*B*) Upper: AAR expressed as a percentage of LV area. Lower: quantification of myocardial infarct size expressed as a percentage of LV AAR ($n = 5–7$, each group). All data were expressed as mean ± SEM. *$P < 0.05$ compared with *Kcne2*$^{+/+}$ mice (by one-way ANOVA). (*C*) Post-IRI mean serum levels of CK, CK-MB, and LDH of *Kcne2*$^{+/+}$ and *Kcne2*$^{-/-}$ mice with ($n = 5–6$) or without SB216763; values for *Kcne2*$^{+/+}$ and *Kcne2*$^{-/-}$ mice without inhibitors are repeated from *Figure 1*, for comparison. *$P < 0.05$, ***$P < 0.001$ compared with *Kcne2*$^{+/+}$ mice (by one-way ANOVA). (*D*) Left: representative TUNEL-stained heart sections of mice in the presence (+) or absence (−) of SB216763 post-surgery. Arrows indicate TUNEL-positive cardiomyocytes (red). Scale bars, 10 μm. Right: graph showing the averaged percentage of TUNEL-positive cells in the ischaemic regions of LVs. Each group: $n = 4–5$. ***$P < 0.001$ compared with *Kcne2*$^{+/+}$ mice (by one-way ANOVA). Values for *Kcne2*$^{+/+}$ and *Kcne2*$^{-/-}$ hearts before SB216763 administration are repeated from *Figure 1H* for comparison.

acute post-ischaemic period, in terms of lessening infarct size and preserving cardiac function.

We also found here that *Kcne2* deletion stimulates ventricular GSK-3β phosphorylation, both at baseline and after IRI (*Figure 4A* and see Supplementary material online, *Figure S2A*). Two of the main pathways known to stimulate phosphorylation of GSK-3β involve AKT phosphorylation—which our results seem to rule out (*Figure 4C* and see Supplementary material online, *Figure S2C*)—and ERK1/2 phosphorylation[20,21] for which there was a ∼50% increase at baseline, albeit considered statistically not significant ($P = 0.27$, *Figure 4B* and $P = 0.11$, see Supplementary material online, *Figure S2B*). It is possible that either ERK phosphorylation is involved in GSK-3β phosphorylation in *Kcne2*$^{-/-}$ mouse ventricles, or a less common pathway is being stimulated, such as the putative one involving GSK-3β phosphorylation via cyclic AMP activation of protein kinase A, or the canonical Wnt pathway[21]—possible targets for follow-up studies. Our observation

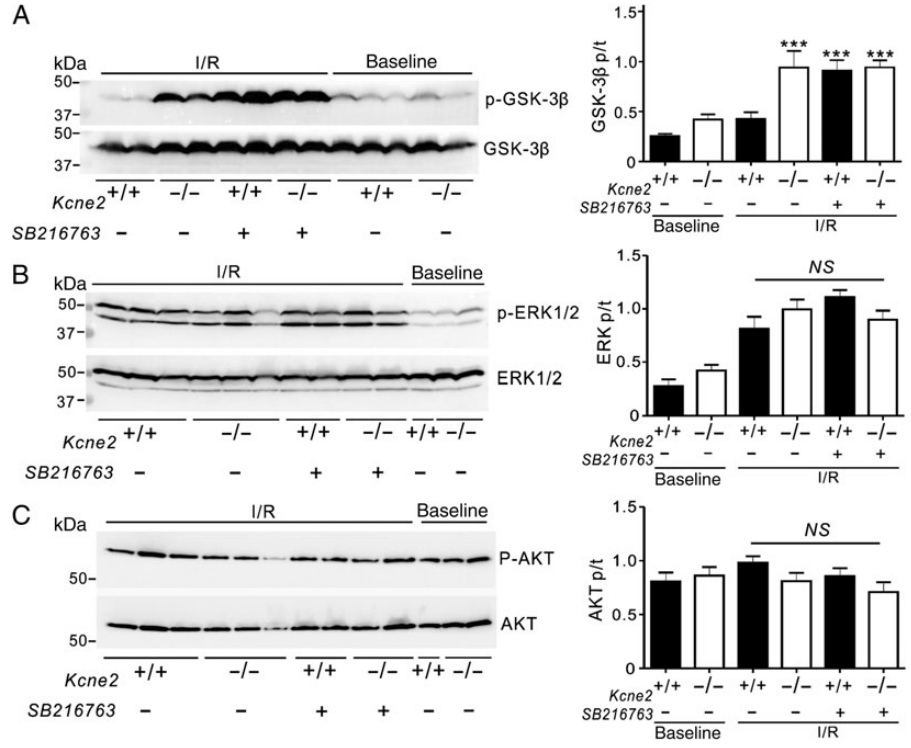

Figure 6 Pharmacological inhibition of GSK-3β upon reperfusion mimics effects of *Kcne2* deletion on GSK-3β phosphorylation. (*A*) Left: representative western blots of phosphorylated GSK-3β and total GSK-3β isolated from ventricles of $Kcne2^{+/+}$ and $Kcne2^{-/-}$ mice in the presence (+) or absence (−) of pharmacological inhibitor SB216763 in baseline and post-IRI. Right: quantification of p-GSK-3β/GSK-3β protein band density; $n = 6–9$, each group. ***$P < 0.0001$ compared with $Kcne2^{+/+}$ with SB216763 (by one-way ANOVA). (*B*) Left: representative western blots of phosphorylated ERK1/2 and total ERK1/2 isolated from ventricles of $Kcne2^{+/+}$ and $Kcne2^{-/-}$ mice in the presence (+) or absence (−) of pharmacological inhibitor SB216763 in baseline and post-IRI. Right: quantification of p- ERK1/2/ERK1/2 protein band density; $n = 4–6$, each group. (*C*) Left: representative western blots of phosphorylated AKT and total AKT isolated from ventricles of $Kcne2^{+/+}$ and $Kcne2^{-/-}$ mice in the presence (+) or absence (−) of pharmacological inhibitor SB216763 in baseline and post-IRI. Right: quantification of p-AKT/AKT protein band density; $n = 4–7$, each group.

that *Kcne2* deletion inactivates ventricular GSK-3β is notable because of the extensive literature linking GSK-3β to ischaemic injury, and GSK-3β inactivation (or inducible knockout) to ischaemic preconditioning.[22] Pharmacological inhibition of GSK activity was previously shown to be cardioprotective in terms of reducing infarct size in various animal models,[23] and inhibition of GSK-3β activity results in the enhancement of its phosphorylation and promotes cell survival.[21]

Importantly, we found that *Kcne2* deletion increases baseline GSK-3β phosphorylation, which may produce a 'cardiac preconditioning'-like phenomenon that protects against subsequent ischaemic insult. GSK-3β phosphorylation in $Kcne2^{-/-}$ mouse ventricles was further increased post-I/R, doubling it compared with post-I/R wild-type littermates. Furthermore, our finding that inactivation of GSK-3β by pretreatment with SB216763 prior to reperfusion did not result in a further increase in GSK-3β phosphorylation or cardioprotection in $Kcne2^{-/-}$ mice, but mimicked in $Kcne2^{+/+}$ mice the degree of GSK-3β phosphorylation and cardioprotection observed in untreated $Kcne2^{-/-}$ mice, is highly supportive of a primary role for GSK-3β phosphorylation (inactivation) in the post-I/R cardioprotection conferred by *Kcne2* deletion. However, inhibition of GSK-3β activity did not alter ERK or AKT phosphorylation post-I/R ($P > 0.05$), suggesting that conventional crosstalk among these signalling pathways was not a crucial factor in the *Kcne2* deletion-specific aspects of post-I/R cardioprotection.

Activated GSK-3β is thought to promote the actions of p53, which stimulates the release of cytochrome *c* and causes disruption of mitochondria during apoptosis,[24] whereas GSK-3β inactivation suppresses mitochondrial permeability transition pore opening, thus preventing cardiomyocyte death.[21] In addition, GSK-3β inactivation prevents its anti-hypertrophic effects,[22] which would be consistent with our previous data, suggesting that *Kcne2* deletion increases heart size at least partly via ventricular hypertrophy (increasing ventricular myocyte size).[10] Interestingly, we also previously found that *Kcne2* deletion causes ventricular fibrosis in 1-year-old mice.[10] In mice with hypertrophic cardiomyopathy, cardiac fibrosis was reportedly mediated by non-myocyte proliferation and both were preventable by chronic angiotensin II receptor antagonism.[25] As *Kcne2* deletion increases serum angiotensin II,[5] which is also known to result in GSK-3β inactivation,[22] it will be of interest to determine the effects in $Kcne2^{-/-}$ mice of angiotensin II receptor antagonism on fibrosis and post-IRI cardioprotection.

It is important to recognize that the magnitude of the response to an experimentally provoked IRI and the susceptibility to naturally occurring infarct-producing IRIs are two fundamentally different parameters. Paradoxically, chronic ischaemia arising from *Kcne2* deletion, stemming from one or more of the combination of impaired glucose tolerance, anaemia, and hypercholesterolaemia and perhaps as yet unknown

defects of this complex mouse model, may contribute to remodelling of the heart in a manner that better prepares it for an acute ischaemic event in the form of an acute IRI. This remodelling limits infarct size, but does not attenuate early reperfusion arrhythmogenesis, which we previously found to be exacerbated by *Kcne2* deletion (probably largely because of delayed myocyte repolarization and hyperkalaemia).[5]

Future studies will be directed towards determining whether *Kcne2* deletion in mice influences the chances of a naturally occurring infarct. This is predicted to be the case because of the risk factors associated with *Kcne2* deletion in mice (including diabetes, anaemia, and hypercholesterolaemia),[5] but we do not yet know whether the reprogramming that limits infarct size after an imposed ischaemic event can also mitigate the effects of the aforementioned risk factors in terms of the chances of a naturally occurring event. This will be particularly important to discern given the association of SNPs in or near human *KCNE2* with CAD/MI, and our recent findings that *Kcne2* deletion promotes atherosclerosis in mice—suggesting that *Kcne2*-disrupted mice would be more likely than wild-type mice to exhibit natural infarcts, especially if placed on a western diet.[15]

Our findings must be interpreted within the constraints of several other potential limitations. (i) human gene mutations or rare SNPs are most commonly represented only on one allele, whereas we examined homozygous *Kcne2*$^{-/-}$ mice, which are at best an exaggeration of the potential human condition because they involve an entire gene deletion from both alleles. (ii) In the current study, we employed an IRI protocol of 45 min of ischaemia followed by 3 h of reperfusion, representing only the acute post-infarct period. A fuller examination of the ultimate infarct outcomes and remodelling (which occurs on an even longer time-frame) will require further investigation, but will be challenging because the many other defects in *Kcne2*$^{-/-}$ mice render them quite frail and difficult to maintain postoperatively. (iii) While no obvious differences in coronary artery anatomy were observed (data not shown), we did not quantify coronary vessel anatomy, genotype-dependent differences which might influence ischaemia (although ST-segment elevation was equivalent between genotypes, suggesting against this) or reperfusion injury. (iv) Importantly, the mouse model we study is a global knockout; therefore, we do not know the relative effects of *Kcne2* deletion from the heart vs. from each of the other tissues in which *Kcne2* is normally expressed, and which effects are beneficial vs. harmful. (v) In the previous study of the effects of *Kcne2* deletion on acute, high-LAD ligation arrhythmogenesis, we studied adult female mice, whereas here we study adult male mice. Direct comparisons between the two studies should therefore be approached with caution because not only the ligation position was different, but also the sex of the mice was different. It will be of interest to determine in future studies whether there is sex-specificity to the GSK-3β-dependent cardioprotection in *Kcne2*$^{-/-}$ mice.

In conclusion, our findings further support the hypothesis that arrhythmia-linked ion channel genes influence a wide spectrum of physiology and pathology outside their established role in conducting ventricular myocyte currents. This diversity of function is important for cardiovascular physiologists and geneticists to acknowledge, because as this and previous studies demonstrate, disruption of arrhythmia susceptibility genes can impact the heart in an unpredictable manner, both deleteriously and, as we show here, with partial benefit in some contexts.

Supplementary material

Supplementary material is available at *Cardiovascular Research* online.

Acknowledgements

We are grateful to Marie Anand, Mou Chen, and Ritu Kant for technical assistance.

Conflict of interest: none declared.

Funding

This work was supported by the National Heart, Lung and Blood Institute at the National Institutes of Health (R01HL079275 and R01HL079275-S1 to G.W.A.) and by the National Natural Science Foundation of China (30901412 to Z.H.).

References

1. George AL Jr. Molecular and genetic basis of sudden cardiac death. *J Clin Invest* 2013;**123**:75–83.
2. Crump SM, Hu Z, Kant R, Levy DI, Goldstein SA, Abbott GW. Kcne4 deletion sex- and age-specifically impairs cardiac repolarization in mice. *FASEB J* 2016;**30**:360–369.
3. Abbott GW. KCNE genetics and pharmacogenomics in cardiac arrhythmias: much ado about nothing? *Expert Rev Clin Pharmacol* 2013;**6**:49–60.
4. Hu Z, Crump SM, Anand M, Kant R, Levi R, Abbott GW. Kcne3 deletion initiates extracardiac arrhythmogenesis in mice. *FASEB J* 2014;**28**:935–945.
5. Hu Z, Kant R, Anand M, King EC, Krogh-Madsen T, Christini DJ, Abbott GW. *Kcne2* deletion creates a multisystem syndrome predisposing to sudden cardiac death. *Circ Cardiovasc Genet* 2014;**7**:33–42.
6. Abbott GW, Sesti F, Splawski I, Buck ME, Lehmann MH, Timothy KW, Keating MT, Goldstein SA. MiRP1 forms IKr potassium channels with HERG and is associated with cardiac arrhythmia. *Cell* 1999;**97**:175–187.
7. Roepke TK, Kanda VA, Purtell K, King EC, Lerner DJ, Abbott GW. KCNE2 forms potassium channels with KCNA3 and KCNQ1 in the choroid plexus epithelium. *FASEB J* 2011;**25**:4264–4273.
8. Roepke TK, Anantharam A, Kirchhoff P, Busque SM, Young JB, Geibel JP, Lerner DJ, Abbott GW. The KCNE2 potassium channel ancillary subunit is essential for gastric acid secretion. *J Biol Chem* 2006;**281**:23740–23747.
9. Roepke TK, Kontogeorgis A, Ovanez C, Xu X, Young JB, Purtell K, Goldstein PA, Christini DJ, Peters NS, Akar FG, Gutstein DE, Lerner DJ, Abbott GW. Targeted deletion of kcne2 impairs ventricular repolarization via disruption of I(K,slow1) and I(to,f). *FASEB J* 2008;**22**:3648–3660.
10. Roepke TK, King EC, Reyna-Neyra A, Paroder M, Purtell K, Koba W, Fine E, Lerner DJ, Carrasco N, Abbott GW. *Kcne2* deletion uncovers its crucial role in thyroid hormone biosynthesis. *Nat Med* 2009;**15**:1186–1194.
11. Roepke TK, King EC, Purtell K, Kanda VA, Lerner DJ, Abbott GW. Genetic dissection reveals unexpected influence of beta subunits on KCNQ1 K^+ channel polarized trafficking in vivo. *FASEB J* 2011;**25**:727–736.
12. Kathiresan S, Voight BF, Purcell S, Musunuru K, Ardissino D, Mannucci PM, Anand S, Engert JC, Samani NJ, Schunkert H, Erdmann J, Reilly MP, Rader DJ, Morgan T, Spertus JA, Stoll M, Girelli D, McKeown PP, Patterson CC, Siscovick DS, O'Donnell CJ, Elosua R, Peltonen L, Salomaa V, Schwartz SM, Melander O, Altshuler D, Merlini PA, Berzuini C, Bernardinelli L, Peyvandi F, Tubaro M, Celli P, Ferrario M, Fetiveau R, Marziliano N, Casari G, Galli M, Ribichini F, Rossi M, Bernardi F, Zonzin P, Piazza A, Yee J, Friedlander Y, Marrugat J, Lucas G, Subirana I, Sala J, Ramos R, Meigs JB, Williams G, Nathan DM, MacRae CA, Havulinna AS, Berglund G, Hirschhorn JN, Asselta R, Duga S, Spreafico M, Daly MJ, Nemesh J, Korn JM, McCarroll SA, Surti A, Guiducci C, Gianniny L, Mirel D, Parkin M, Burtt N, Gabriel SB, Thompson JR, Braund PS, Wright BJ, Balmforth AJ, Ball SG, Hall AS, Linsel-Nitschke P, Lieb W, Ziegler A, Konig I, Hengstenberg C, Fischer M, Stark K, Grosshennig A, Preuss M, Wichmann HE, Schreiber S, Ouwehand W, Deloukas P, Scholz M, Cambien F, Li M, Chen Z, Wilensky R, Matthai W, Qasim A, Hakonarson HH, Devaney J, Burnett MS, Pichard AD, Kent KM, Satler L, Lindsay JM, Waksman R, Knouff CW, Waterworth DM, Walker MC, Mooser V, Epstein SE, Scheffold T, Berger K, Huge A, Martinelli N, Olivieri O, Corrocher R, McKeown P, Erdmann E, Konig IR, Holm H, Thorleifsson G, Thorsteinsdottir U, Stefansson K, Do R, Xie C, Siscovick D. *Genome-wide association of early-onset myocardial infarction with single nucleotide polymorphisms and copy number variants. Nat Genet* 2009;**41**:334–341.
13. Sabater-Lleal M, Malarstig A, Folkersen L, Soler Artigas M, Baldassarre D, Kavousi M, Almgren P, Veglia F, Brusselle G, Hofman A, Engstrom G, Franco OH, Melander O, Paulsson-Berne G, Watkins H, Eriksson P, Humphries SE, Tremoli E, de Faire U, Tobin MD, Hamsten A. Common genetic determinants of lung function, subclinical atherosclerosis and risk of coronary artery disease. *PLoS ONE* 2014;**9**:e104082.

14. Wakil SM, Ram R, Muiya NP, Mehta M, Andres E, Mazhar N, Baz B, Hagos S, Alshahid M, Meyer BF, Morahan G, Dzimiri N. A genome-wide association study reveals susceptibility loci for myocardial infarction/coronary artery disease in Saudi Arabs. *Atherosclerosis* 2016;**245**:62–70.
15. Lee SM, Nguyen D, Hu Z, Abbott GW. *Kcne2* deletion promotes atherosclerosis and diet-dependent sudden death. *J Mol Cell Cardiol* 2015;**87**:148–151.
16. Mitchell GF, Jeron A, Koren G. Measurement of heart rate and Q-T interval in the conscious mouse. *Am J Physiol* 1998;**274**(3 Pt 2):H747–H751.
17. Ko SH, Yu CW, Lee SK, Choe H, Chung MJ, Kwak YG, Chae SW, Song HS. Propofol attenuates ischemia-reperfusion injury in the isolated rat heart. *Anesth Analg* 1997;**85**: 719–724.
18. Szpakowicz A, Kiliszek M, Pepinski W, Waszkiewicz E, Franaszczyk M, Skawronska M, Dobrzycki S, Niemcunowicz-Janica A, Ploski R, Opolski G, Musial WJ, Kaminski KA. *The rs9982601 polymorphism of the region between the SLC5A3/MRPS6 and KCNE2 genes associated with a prevalence of myocardial infarction and subsequent long-term mortality. Pol Arch Med Wewn* 2015;**125**:240–248.
19. Ou L, Li W, Liu Y, Zhang Y, Jie S, Kong D, Steinhoff G, Ma N. Animal models of cardiac disease and stem cell therapy. *Open Cardiovasc Med J* 2010;**4**:231–239.
20. Sugden PH, Fuller SJ, Weiss SC, Clerk A. Glycogen synthase kinase 3 (GSK3) in the heart: a point of integration in hypertrophic signalling and a therapeutic target? A critical analysis. *Br J Pharmacol* 2008;**153**(Suppl 1):S137–S153.
21. Miura T, Miki T. GSK-3beta, a therapeutic target for cardiomyocyte protection. *Circ J* 2009;**73**:1184–1192.
22. Cheng H, Woodgett J, Maamari M, Force T. Targeting GSK-3 family members in the heart: a very sharp double-edged sword. *J Mol Cell Cardiol* 2011;**51**:607–613.
23. Rose BA, Force T, Wang Y. Mitogen-activated protein kinase signaling in the heart: angels versus demons in a heart-breaking tale. *Physiol Rev* 2010;**90**: 1507–1546.
24. Watcharasit P, Bijur GN, Song L, Zhu J, Chen X, Jope RS. Glycogen synthase kinase-3 beta (GSK3beta) binds to and promotes the actions of p53. *J Biol Chem* 2003;**278**: 48872–48879.
25. Teekakirikul P, Eminaga S, Toka O, Alcalai R, Wang L, Wakimoto H, Nayor M, Konno T, Gorham JM, Wolf CM, Kim JB, Schmitt JP, Molkentin JD, Norris RA, Tager AM, Hoffman SR, Markwald RR, Seidman CE, Seidman JG. Cardiac fibrosis in mice with hypertrophic cardiomyopathy is mediated by non-myocyte proliferation and requires Tgf-beta. *J Clin Invest* 2010;**120**:3520–3529.